Future Generation Computer Systems 113 (2020) 70–77

Contents lists available at ScienceDirect

Future Generation Computer Systems

journal homepage: www.elsevier.com/locate/fgcs

A decision support system using hybrid AI based on multi-image quality model and its application in color design

Mengshan Li *, Suyun Lian, Fan Wang, Yanying Zhou, Bingsheng Chen, Lixin Guan, Yan Wu

College of Physics and Electronic Information, Gannan Normal University, Ganzhou, Jiangxi 341000, China

ARTICLE INFO

Article history:
Received 6 March 2020
Received in revised form 20 June 2020
Accepted 23 June 2020
Available online 3 July 2020

Keywords:
Decision support system
Artificial intelligence
Product design
Multi-users' images

ABSTRACT

The product-color image conveys consumers' color demands through emotion cognition. In this paper, a decision support system is proposed based on the hybrid artificial intelligence algorithm. The proposed system explores the internal correlation between the color image and demand of users. In the proposed system, an artificial neural network based on the radial basis function is employed. The network model is trained with an improved particle swarm optimization combined with the weight-adaptive strategy and chaos theory. The proposed model predicts the multi-uses' color images. Then, the decision colors are extracted from the predicted colors by K-harmonic means clustering. The experimental results show that the proposed color decision support system is promising in designing the color scheme and providing theoretical guidance for the product-color design.

1. Introduction

The product-color image is defined as consumers' intuitive association with product-color, which fully conveys consumer's demand for the color. The product-color image is of theoretical and practical value because it affects consumer's decisions in the purchase, and designers can understand customers' color emotion cognition by it [1]. The design of a product-color has been transformed from the traditional experience-based strategy to the user-centered decision strategy. Before the designers grasp users' image preference and cognition to product-color and reduce the perception gap with the users in the color image, they cannot design the products conforming to users' images or improve the design [2,3].

Previous studies on product-color design were based on color harmony theory, knowledge-engineering theory, and customers' images obtained with intelligent computation. Traditional color design methods failed to meet diverse and changeable demands since the fuzzy perceptual description of the color image was not considered. Thus, understanding the consumer's complex perceptual images of product-color has become a significant element in product-color design [4].

In recent years, many product-color design methods were proposed based on intelligent computation, such as gray theory [5,6], fuzzy theory, support vector machine (SVM) [7,8], artificial neural network (ANN) [9–13], and imperialist competitive algorithm. Also, several methods were proposed based on the various swarm intelligence algorithms, such as tabu search algorithm, ant colony algorithm, genetic algorithm, and particle swarm optimization algorithm, which were successfully applied in various product designs [14–16]. As a novel design method imitating color evolution under the influence of the law of survival of the fittest in biological evolution, the swarm intelligence-based product-color design has played an important role [17,18]. For example, Hsiao et al. used the gray theory and backpropagation artificial neural network (BP ANN) to study the color of baby walker, proving that the gray theory prediction model can be applied in the color design of all kinds of products [19–21]. In [6,19,22–25], the double-color system for the product-color design was proposed based on the gray theory, color harmony method, and genetic algorithm. The genetic algorithm was applied and verified in the product-color selection [20,21,26–29]. Shiu [30] used the artificial neural network to establish the color prediction model in the study of the color of children's toys. Chen et al. [31] established the color image base by using user preference as the input value.

However, previous studies mostly focused on the application of intelligent computing algorithms only in the development process of the color scheme. Users' color image was not considered as the main factor in the studies on color selection. The only single-user rather than mass-users was considered in the design process, leading the dotted distribution problem. Also, intelligent computation algorithms had problems, such as the artificial neural network might lead to unstable results because of the uncertainty of the initial values of parameters and the weight. Swarm intelligence algorithms also had some problems, such as

* Corresponding author.
E-mail address: jcimsli@163.com (M. Li).

https://doi.org/10.1016/j.future.2020.06.034
0167-739X/

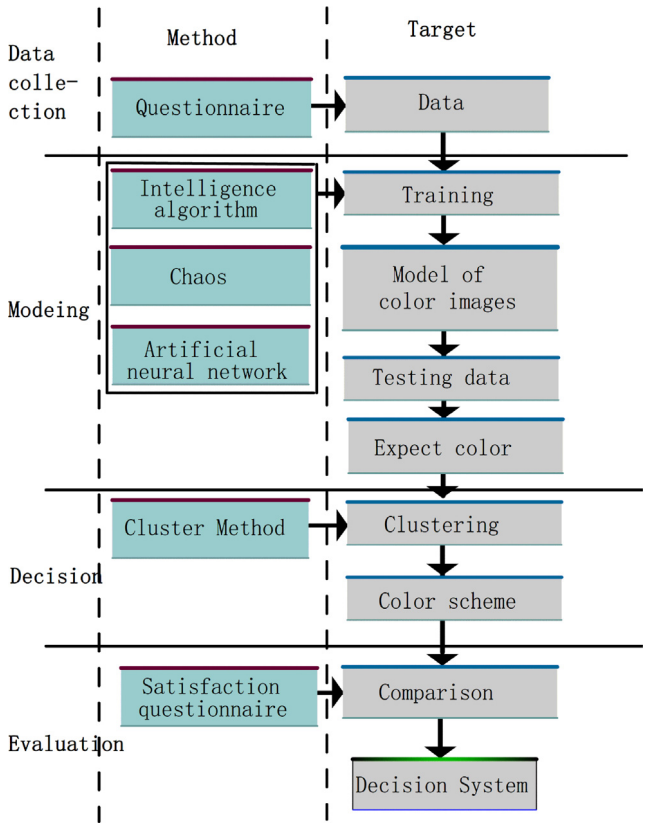

Fig. 1. The diagram of the proposed system.

premature convergence and slow local search, which seriously affected the reliability of the product-color decision.

To solve the above problems, it is necessary to accurately and efficiently grasp the complex emotional images of the overall consumption group for product-color. In this paper, we propose the product-color decision system based on the hybrid intelligent method and multi-users' color images. In the system, multi-users' data were fused in order to solve the dotted distribution problem, and multi-user color images were used as the main factor to express the user color perception. Further, various intelligent methods were integrated to overcome some disadvantages of the traditional evolutionary algorithm.

2. System model and theory

2.1. The process of the proposed system

In this paper, we propose a hybrid product-color decision system based on chaos theory, intelligence algorithm, clustering method, and artificial neural network. The diagram of the proposed system is shown in Fig. 1.

The proposed system is consists of four steps: (i) data collection, (ii) the expected color prediction model, (iii) expected color decision, and (iv) evaluation.

(1) Data collection.

In order to obtain the users' expected color images of products, a sample database was established through the questionnaire.[1]

(2) The prediction model for the expected color.

Due to the fuzziness of color image, the relationship between expected color and color image is nonlinear. In order to model the complicated relation, Radial Basis Function Artificial Neural Network (RBF-ANN) is employed, which predicts the expected colors trained by a swarm intelligence algorithm. In the swarm intelligence algorithm, the inertia weight was adjusted by adaptive strategy, the cognitive factor and exploration factor were obtained with the Lorenz chaotic sequence.

(3) Color decision based on K-harmonic-means clustering.

Many expected colors were obtained in the modeling process, but few of them are adopted in the production process. An essential task is to recommend the production colors, which represent the users' expectations. In this paper, the K-harmonic-means clustering method is adopted to divide the predicted colors into several categories. Those colors in the same category were close or similar, so they were considered to be the same color series during the color decision.

(4) Evaluation of the decision color

In order to evaluate the user's satisfaction with the recommended colors in the decision process, we established a satisfaction questionnaire. A higher degree of satisfaction indicates that the color decision system is working well.

The proposed color decision system aims to establish the mapping model between color image and expected color through hybrid artificial intelligence techniques based on the perspective of multi-users' images and get the final color scheme with the clustering method. Multi-users' images are mainly manifested in two aspects. First, the prediction model is based on multi-user inputs (product-color images) and outputs (expected colors). Second, the color scheme is based on multi-users' comprehensive expected colors. System intelligence is also reflected in two aspects. First, the combination of chaos theory and artificial neural network makes the prediction model more intelligent. Second, the automatic clustering of the expected colors allows the color scheme.

2.2. Artificial neural network model based on hybrid intelligent method

2.2.1. Radial basis function artificial neural network

RBF-ANN is one of the most widely used forward neural network models, whose structure consists of three layers: the input layer, hidden layer, and output layer. The Gauss activation function is adopted in this paper and defined as follows:

$$g_i(x_k) = \exp(-\frac{\|x_k - c_i\|^2}{\sigma_i^2}), \tag{1}$$

where $x_k (1 \le k \le n)$ is the kth output vector and $c_i (1 \le i \le c)$ is the basis function center. n and c are the number of samples and the number of hidden nodes, respectively. σ_i is the spreading constant. The network output layer is defined as:

$$O(x_k) = \sum_{i=1}^{c} w_i g_i(x_k), \tag{2}$$

where w_i is the connection weight of the ith hidden node.

The performance is directly related to the optimization of the network weight. The training process of RBF-ANN is the optimization process of the base function center, spreading constant and connection weight, namely, c_i, σ_i, w_i. Various algorithms have been applied in the network training, such as genetic algorithm, particle swarm optimization (PSO), and fish-swarm algorithm. PSO is a typical heuristic swarm intelligence algorithm and widely applied due to its fast convergence, simple parameter adjustment, and easy implementation [32–34]. However, PSO algorithm does not guarantee the optimal solution in each execution. In this paper, the improved PSO algorithm was proposed based on the adaptive weight strategy and the chaos theory.

[1] Please refer to the Appendix for the questionnaire details used in this paper.

2.2.2. Improved PSO algorithm

PSO has been widely used due to its advantages, such as structural simplicity, a small number of parameters, ease of implementation, global search capability, and non-requirement of gradient information. In the standard PSO search process, each particle is regarded as a potential solution. The speed and location of particles are defined as (3) and (4), respectively.

$$v_{i,d}^{k+1} = \omega v_{i,d}^{k} + c_1(p_{i,d}^{k} - x_{i,d}^{k}) + c_2(p_{g,d}^{k} - x_{i,d}^{k}), \tag{3}$$

$$x_{i,d}^{k+1} = x_{i,d}^{k} + v_{i,d}^{k+1}, \tag{4}$$

where $x_{i,d}^{k}$ and $v_{i,d}^{k}$ represent the location of the ith particle and the speed at the time k, respectively, in the dth dimension. $i = 1, \ldots, m$ where m is the number of population particles. ω is the inertia weight. c_1 and c_2 are the acceleration factors, respectively. $p_{i,d}^{k}$ and $p_{g,d}^{k}$ are the local extrema of the particle and the global extrema of the population, respectively.

Particle velocity is determined by three factors: (1) inertia weight factor, which shows that the relationship between the current and previous speed; (2) cognitive factor, which represents the exploitation of the capacity factor and indicates the relationship of the optimal particle with itself; (3) exploration factor, which is the social sharing coefficient representing the optimal correlative degree. The inertia coefficient is conducive to global search when it is high and to local search when it is low. Cognitive and exploration factors are collectively called the learning factor. When both are adjusted, they can evaluate the search speed of the particles in the global and local topologies, thereby contributing to the improvement of convergence speed and accuracy. Thus, this paper adopted the adaptive weight strategy and chaos theory to prevent premature convergence and the local extrema problem of the algorithm. The adjusting function of the inertia weight is defined as follows:

$$\omega = \omega_{\max} - Pgbest(k)/Plbest_{ave} - (\omega_{\max} - \omega_{\min}) \times k/k_{\max} \tag{5}$$

where $\omega_{\max}$ and $\omega_{\min}$ are the maximum and minimum inertia weights, respectively. $Pgbest(k)$ and $Plbest_{ave}$ indicate the global extrema value and average local extrema value, respectively. k and $k_{\max}$ are the current and maximum number of iterations, respectively.

The accelerating factors c_1 and c_2 are obtained with the chaotic sequence generated by the Lorenz chaos equation, defined as follows:

$$\begin{cases} \dfrac{dx}{dt} = -a(x - y) \\ \dfrac{dy}{dt} = rx - y - xz \\ \dfrac{dz}{dt} = xy - bz \end{cases}, \tag{6}$$

where a, b, and r are the system parameters. When a, b, and r are set to be 10, 8/3, and 28, the system is in the fully chaotic state. The accelerating factors c_1 and c_2 are defined as:

$$\begin{cases} c_1 = x(t) \\ c_2 = y(t) \end{cases} \tag{7}$$

Chaotic variables are characterized by their randomness, ergodicity, and regularity. By changing the characteristics of chaotic variables, the algorithm can simultaneously increase the diversity of the population and improve the premature convergence problem.

2.2.3. RBF-ANN based on the hybrid intelligent method

Three parameters of RBF-ANN, namely c_i, σ_i, w_i, are optimized through the above hybrid training method. The structure of the particle is defined as:

$$particle(i) = [W_{h,o}, B_{h,o}, C_{basis-fun}] \tag{8}$$

where $W_{h,o}$ and $B_{h,o}(1 \le h \le c)$, $(1 \le o \le p)$ are the weight matrix and deviation matrix of the hidden node h and the output node o, respectively. $C_{basis-function}$ is the base function center and $KHM(X, C) = \sum_{i=1}^{n} \frac{k}{\sum_{j=1}^{k} \frac{1}{\|x_i - c_j\|^p}}$ is the number of output nodes.

2.3. Clustering-based multi-user color decision scheme

A multi-user decision is an effective way for the overall system evaluation. In the process of product-color decision, it is only required to get several representative colors satisfying the public, but multiple users have several different color expectations. Selecting the more representative color is the key to the decision scheme. In this paper, we used K-harmonic-means (KHM) for the clustering decision of the color expectations.

KHM clustering is conducted in the iteration process based on cluster centers. The objective function adopts the harmonic mean from all sample points to all cluster centers, defined as follows:

$$KHM(X, C) = \sum_{i=1}^{n} \frac{k}{\sum_{j=1}^{k} \frac{1}{\|x_i - c_j\|^p}}, \tag{9}$$

where $X = [x_1, \ldots, x_n]$ is the sample database. n and k are the number of samples and the number of clusters, respectively. $C = [c_1, \ldots, c_n]$ is the central vector of the cluster.

The degree of membership $m(c_j/x_i)$ and the weight $w(x_i)$ of each sample data x_i are computed as (10) and (11).

$$m(c_j/x_i) = \frac{\|x_i - c_j\|^{-p-2}}{\sum_{j=1}^{k} \|x_i - c_j\|^{-p-2}} \tag{10}$$

$$w(x_i) = \frac{\sum_{j=1}^{k} \|x_i - c_j\|^{-p-2}}{(\sum_{j=1}^{k} \|x_i - c_j\|^{-p})^2} \tag{11}$$

where p is the output parameter and set to be 2 in this paper. The central vector of cluster c_j is computed as follows:

$$c_j = \frac{\sum_{i=1}^{n} m(c_j/x_i) w(x_i) x_i}{\sum_{i=1}^{n} m(c_j/x_i) w(x_i)} \tag{12}$$

In the KHM clustering algorithm, the objective function gradually decreases to obtain a stable value with interactions according to the central vector.

3. Case study

In this section, we study the exterior color of the compact hatchback car. The target users of the case study are young people aged 25 to 35 for whom the car is not only a means of transport but also a carrier reflecting their personalities. Note that the influences of color matching, materials, and decorative parts are not considered.

3.1. Dataset

Through expert interviews and analysis of benchmarking cars, forty words were obtained that are used for describing the user's image on the compact hatchback car. The full list of words is shown in Table 1.

From the color system commonly used in the automobile design industry, 50 representative exterior color samples were selected through expert interviews. The color samples are shown in Fig. 2.

A questionnaire was compiled with 40 image words and 50 color samples. Each participant was asked to select the expected automobile exterior colors and score how the words correspond

Table 1
Users' image color words.

No.	Word	No.	Word	No.	Word	No.	Word	No.	Word
01	Local	02	International	03	Fashionable	04	Avant-garde	05	Streamline
06	Muscle	07	Simple	08	Luxurious	09	Household	10	Business
11	Fine	12	Rough	13	Solid	14	Swift	15	Graceful
16	Elegant	17	Soft	18	Tough	19	Natural	20	Science
21	Classic	22	Modern	23	Traditional	24	Advanced	25	Masculine
26	Feminine	27	Implicit	28	Aggressive	29	Relaxed	30	Pressing
31	Silent	32	Active	33	Affinitive	34	Aloof	35	Dim
36	Striking	37	Steady	38	Brisk	39	Urban	40	Suburb

Fig. 2. The commonly used color samples in the automobile design industry.. (For interpretation of the references to color in this figure legend, the reader is referred to the web version of this article.)

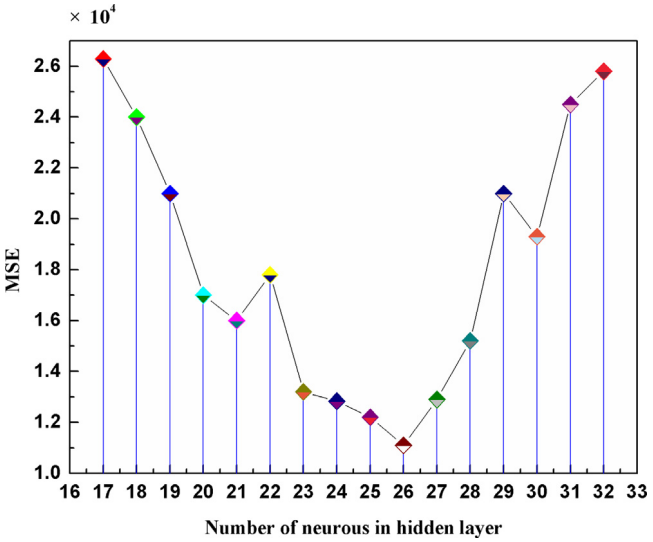

Fig. 3. The prediction errors according to the number of nodes in the hidden layer.

to the expected colors. The five-level of scores are used where 1 indicates the weak, while 5 represents the very-strong. (Please refer to the Appendix for the detailed questionnaire.)

The survey was conducted with 723 participants who are young people aged 25 to 35 with healthy eyesight and sense of color. Redundant and unsuitable questionnaires were screened out so that 628 valid questionnaires were obtained to construct the database for the automobile exterior color image. The database is divided into three sub-datasets: (1) training set is used to train the parameters of the network, (2) the validation set is used to validate the accuracy and pick the epoch of the model being trained, and (3) the test set is used to test the performance of the model. The optimal data distribution is empirically determined as 70% (440), 15% (94), and 15% (94) for the training, validation, and test datasets, respectively.

3.2. System model

The RBF-ANN model, based on a hybrid intelligent method, was used in the experiments. The input to the RBF-ANN model is 40 color words, while the output of the model is the corresponding expected colors in three channels of Lab color space. The number of nodes in the hidden layer is determined by experiments. The initial number of nodes is determined with the formula: $2 * \text{sqrt}(m * n) + 1$, where m and n are the numbers of nodes in the input layer and the output layer, respectively. For the hidden layer, 23 nodes are initially set. Then, the performance was experimentally tested with the number of nodes being changed from 17 to 32. Fig. 3 shows the prediction errors according to the number of nodes in the hidden layer. As shown in Fig. 3, the smallest errors were obtained with 26 nodes. Consequently, the model consists of 40, 26, and 3 nodes for the input, hidden, and output layers, respectively.

The color difference is used to describe the similarity between the two colors. Chromatic values of (L_1^*, a_1^*, b_1^*) and (L_2^*, a_2^*, b_2^*) in CIELab color space are used to define the color difference ΛE:

$$\Lambda E = \sqrt{(L_1^* - L_2^*)^2 + (a_1^* - a_2^*)^2 + (b_1^* - b_2^*)^2} \tag{13}$$

The smaller value indicates similar colors. Note that ΛE less than 1 means they can be considered to be the same color. Also note that if ΛE is less than 2.3, they are difficult to be distinguished from each other by the human visual system (known as Just Noticeable Difference).

3.3. Results and discussion

3.3.1. Results of the proposed model

The input data is $440 * 40$, and the output data is $440 * 3$ for the training dataset, while the input data is $94 * 40$, and the output data is $94 * 3$ for the validation and test datasets. Figs. 4 and 5 show the color difference between the computed and the ground-truth colors in the training and validation subsets, respectively.

In the training subset (Fig. 4), the average value of the color differences is about 2, where most ones are less than 2.3 while a few ones are higher than 3. In the validation subset (Fig. 5), the average value of the color differences is about 1.6, where most ones are less than 1.6. Further, many samples are predicted with a difference of less than 1 in both the training and validation subsets. Fig. 6 shows the color difference in the test subset. Most of the differences are less than 3, indicating that the predicted colors are consistent with the users' expected colors. As described in Section 3.2, the difference of less than 1 is considered consistent with the ground-truth. Also, the difference of less than

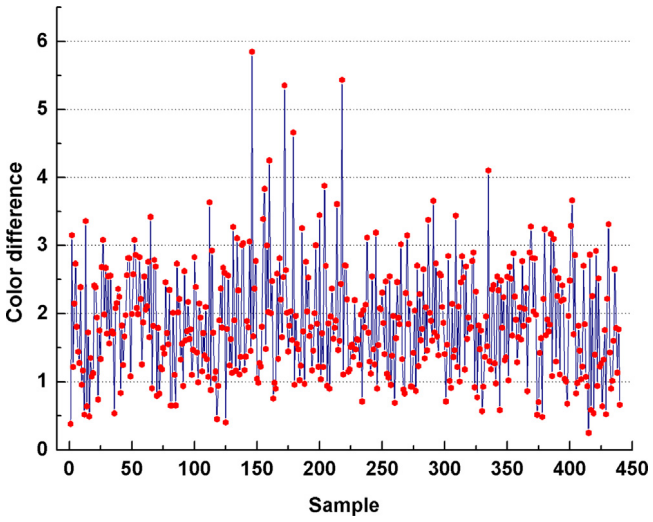

Fig. 4. Color difference distribution in the training set.

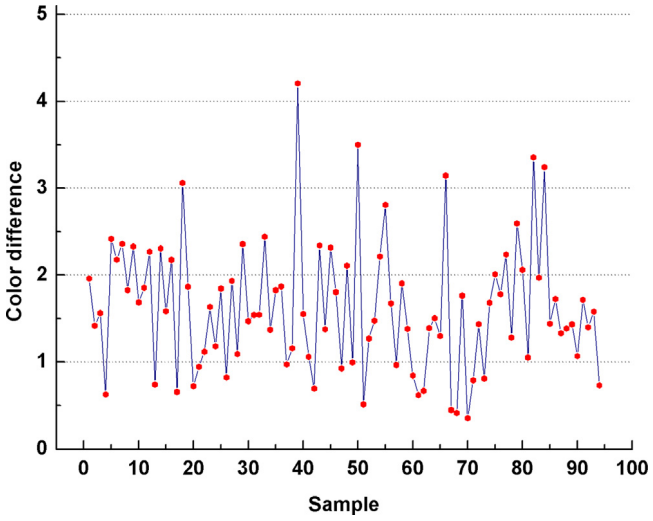

Fig. 5. Color difference distribution in the validation set.

Table 2
Statistics of the prediction errors of the proposed model.

Dataset	Average ΔE	Min ΔE	Max ΔE	$\Delta E < 2.3$	$\Delta E < 2$	$\Delta E < 1$
Training	1.8731	0.2524	5.8477	90.011%	60.682%	13.864%
Validation	1.6205	0.3551	4.2069	91.432%	74.468%	22.340%
Testing	2.0952	0.5307	5.6750	81.331%	52.128%	11.702%
Average	1.8630	0.3794	5.2432	87.591%	61.465%	14.809%

2.3 is considered a negligible error in the human visual system. Thus, the results show that the proposed model provides accurate prediction and, consequently, a promising potential in the color decision application.

Table 2 summarizes the color differences of the proposed model for the training, validation, and test subsets. The proposed model showed the best overall performance in the validation subset in terms of the percentage of low errors and the average color difference. Overall, Average ΔE is 1.863 and $\Delta E < 2.3$ is 87%, showing excellent color prediction performance in all subsets.

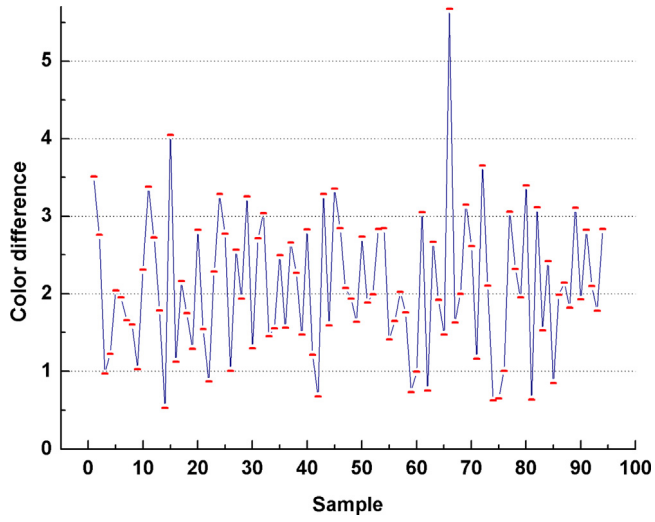

Fig. 6. Color difference distribution in the test set.

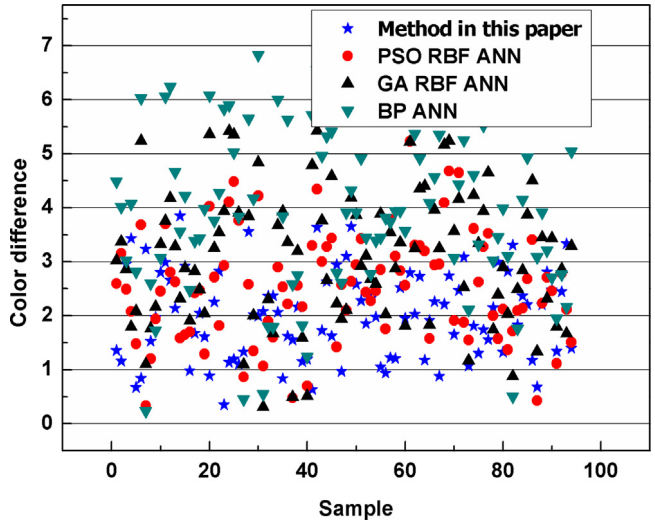

Fig. 7. Color difference distribution of the comparison models.. (For interpretation of the references to color in this figure legend, the reader is referred to the web version of this article.)

3.3.2. Comparisons to other models

To verify the performance of the proposed model, three well-known models, backpropagation artificial neural networks (BP-ANN), PSO-RBF-ANN, and Genetic Algorithm-based RBF-ANN (GA-RBF-ANN), were employed as comparative models. Fig. 7 describes the color difference distribution for different models.

As depicted in Fig. 7, the proposed model provides lower color differences than those of PSO-RBF-ANN, GA-RBF-ANN, and BP-ANN. Table 3 shows the comparison of the models in the test dataset. The results show that the proposed model gives the best accuracy in terms of the Average ΔE, $\Delta E < 2.3$, $\Delta E < 2$, and $\Delta E < 1$.

3.3.3. Analysis of color clustering

Usually, one automobile design has limited exterior colors due to some limitations, such as costs. The output 94 predicted colors are too complicated and do not meet the design requirements. Therefore, we need to decide a few colors satisfying most users. Some predicted colors can be considered the same category

Table 3
Comparisons of the prediction errors for different models.

Dataset	Average ΔE	Min ΔE	Max ΔE	$\Delta E < 2.3$	$\Delta E < 2$	$\Delta E < 1$
BP-ANN	2.8954	0.5483	6.8103	69.853%	40.443%	6.365%
PSO-RBF-ANN	2.3487	0.5438	4.4467	75.123%	49.123%	9.978%
GA-RBF-ANN	2.3564	0.5573	5.1139	75.212%	48.375%	9.326%
The proposed model	2.0952	0.5307	5.6750	81.373%	52.128%	11.702%

Table 4
The statistics of the predicted color clustering.

Clusters	Number	ΔE min	Color			
			ID	L	A	B
Cluster 1	9	0.8677	101	53.9213	71.8975	64.8580
Cluster 2	14	0.6262	102	99.6796	−0.4233	−0.3321
Cluster 3	10	0.6525	103	0.3530	0.5418	0.0873
Cluster 4	19	0.5307	104	81.8033	−0.3252	0.3704
Cluster 5	4	1.9512	105	37.8196	38.4851	48.5341
Cluster 6	7	1.1238	106	63.5940	−13.1161	−30.6411
Cluster 7	8	0.6791	107	87.1461	3.9296	73.3406
Cluster 8	4	2.0214	108	5.3417	16.1057	−36.6631
Cluster 9	5	1.9374	109	75.1315	−29.9235	61.4934
Cluster 10	9	1.8877	110	23.0784	26.6638	−30.1441
Cluster 11	5	3.0388	111	60.2279	10.9768	29.9390

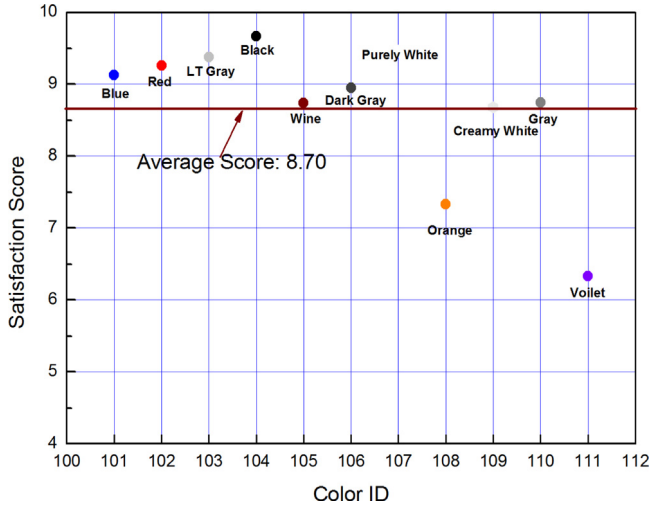

Fig. 8. Evaluation of user satisfaction for the provided colors.

of colors so that the number of colors can be reduced a lot. For this, the KHM clustering algorithm is applied to cluster 94 predicted colors. The clustering results are shown in Table 4. According to the clustering results, 11 types of colors were obtained, where they have high intra-cluster similarity and inter-cluster differences. A representative color is selected with the smallest difference from expected colors.

3.3.4. Satisfaction analysis

This section evaluates user satisfaction on the colors provided by the proposed system given. The questionnaire for user satisfaction has complied with a scale: 1 to 10, where 1 represents *very dissatisfactory* while 10 represents *very satisfactory*. In the survey, 106 participants were asked to rate the satisfaction, who are young people aged 25 to 35. Fig. 8 presents the average value of user satisfaction for each color. Average satisfaction is 8.70, and several colors achieved more than 9 points.

The automobile exterior colors are mainly divided into eternal colors and fashion-exploring colors. Among the colors with high satisfaction, 101 (blue), 102 (red), 103 (LT gray), 104 (black), and 107 (white) colors obtained more than 9 points on color satisfaction. These colors were all popular external colors with high satisfaction. Also, 109 and 110 colors were close to gray and creamy white with high satisfaction, indicating that those fashion-exploring colors could be popular in the future. The 111 color (close to violet) obtained low satisfaction of 0.6 points.

In the color design with the color decision system, the decision-makers can take the external colors with high user satisfaction as the mainstream color at present and take the exploring colors as the future color preferences. Also, they can adopt those with low customer satisfaction as the personality display colors for the minority.

4. Conclusions

This paper proposes an intelligent color decision system based on the evolutionary algorithm, clustering, and artificial neural network. The case study of the automobile exterior colors verified the performance of the proposed model, showing that the decided colors lead to high customer satisfaction. The study can assist the designers to rapidly create the colors satisfying the users and provide new ideas for color design.

(1) The proposed model can better reflect the demands and changes of the whole market as well as the distribution characteristics of multi-users' demands, thus improving the efficiency and quality of color design.

(2) The proposed model can be used in the selection of both primary and secondary exterior colors of the automobile. It can also be used in color matching based on color esthetics, color matching area, and other theories.

(3) The proposed model leads to accurate and fast product-color design by solving the nonlinear mapping problem between multi-users' color images and expected colors.

Future works will include the analysis of multi-users' preferences based on the consideration of age, gender, and other characteristics.

Declaration of competing interest

The authors declare that they have no known competing financial interests or personal relationships that could have appeared to influence the work reported in this paper.

Acknowledgments

The authors gratefully acknowledge the support from the National Natural Science Foundation of China (Grant Numbers: 51663001) and the science and technology research project of the education department of Jiangxi province, China (Grant Numbers: GJJ180773, GJJ180754).

References

[1] F. Xiao, J. Fan, G.S. Chen, J.L. Hulsey, Bridge health monitoring and damage identification of truss bridge using strain measurements, Adv. Mech. Eng. 11 (2019).

[2] M. Smolik, V. Skala, Large scattered data interpolation with radial basis functions and space subdivision, Integr. Comput.-Aided Eng. 25 (2018) 49–62.

[3] S. Liu, Q. Li, J. Liu, W. Chen, Y. Zhang, A realization method for transforming a topology optimization design into additive manufacturing structures, Engineering 4 (2018) 277–285.

[4] G. Rong, A. Mendez, E. Bou Assi, B. Zhao, M. Sawan, Artificial intelligence in healthcare: Review and prediction case studies, Engineering (2020).
[5] A. Mohebbi, S. Achiche, L. Baron, Integrated and concurrent detailed design of a mechatronic quadrotor system using a fuzzy-based particle swarm optimization, Eng. Appl. Artif. Intell. 82 (2019) 192–206.
[6] S.W. Hsiao, C.H. Lee, R.Q. Chen, C.H. Yen, An intelligent system for fashion colour prediction based on fuzzy C-means and gray theory, Color Res. Appl. 42 (2017) 273–285.
[7] J. Chen, Q. Hu, X. Xue, M. Ha, L. Ma, Support function machine for set-based classification with application to water quality evaluation, Inform. Sci. 388 (2017) 48–61.
[8] M.S. Li, H.J. Zhang, L. Liu, B.S. Chen, L.X. Guan, Y. Wu, A quantitative structure-property relationship model based on chaos-enhanced accelerated particle swarm optimization algorithm and back propagation artificial neural network, Appl. Sci. 8 (2018) 1121.
[9] X. Qi, G. Chen, Y. Li, X. Cheng, C. Li, Applying neural-network-based machine learning to additive manufacturing: Current applications, challenges, and future perspectives, Engineering 5 (2019) 721–729.
[10] B.H. Si, J.G. Wang, X.Y. Yao, X. Shi, X. Jin, X. Zhou, Multi-objective optimization design of a complex building based on an artificial neural network and performance evaluation of algorithms, Adv. Eng. Inform. 40 (2019) 93–109.
[11] S. Van Loy, K. Binnemans, T. Van Gerven, Mechanochemical-assisted leaching of lamp phosphors: A green engineering approach for rare-earth recovery, Engineering 4 (2018) 398–405.
[12] S. Itani, F. Lecron, P. Fortemps, Specifics of medical data mining for diagnosis aid: A survey, Expert Syst. Appl. 118 (2019) 300–314.
[13] D. Valdes-Ramirez, M.A. Medina-Perez, R. Monroy, O. Loyola-Gonzalez, J. Rodriguez, A. Morales, F. Herrera, A review of fingerprint feature representations and their applications for latent fingerprint identification: Trends and evaluation, IEEE Access 7 (2019) 48484–48499.
[14] M.S. Li, H.J. Zhang, B.S. Chen, Y. Wu, L.X. Guan, Prediction of pKa values for neutral and basic drugs based on hybrid artificial intelligence methods, Sci. Rep. 8 (2018) 3991.
[15] B. Fielding, L. Zhang, Evolving image classification architectures with enhanced particle swarm optimisation, IEEE Access 6 (2018) 68560–68575.
[16] M. Mousavi, H.J. Yap, S.N. Musa, F. Tahriri, S.Z. Md Dawal, Multi-objective AGV scheduling in an FMS using a hybrid of genetic algorithm and particle swarm optimization, PLoS One 12 (2017) e016981.
[17] S.W. Hsiao, C.F. Hsu, K.W. Tang, A consultation and simulation system for product color planning based on interactive genetic algorithms, Color Res. Appl. 38 (2013) 375–390.
[18] P.P. Plehiers, S.H. Symoens, I. Amghizar, G.B. Marin, C.V. Stevens, K.M. Van Geem, Artificial intelligence in steam cracking modeling: A deep learning algorithm for detailed effluent prediction, Engineering 5 (2019) 1027–1040.
[19] S.W. Hsiao, C.H. Lee, R.Q. Chen, C.Y. Lin, A methodology for brand feature establishment based on the decomposition and reconstruction of a feature curve, Adv. Eng. Inform. 38 (2018) 14–26.
[20] S.W. Hsiao, C.H. Yen, C.H. Lee, An intelligent skin-color capture method based on fuzzy C-means with applications, Color Res. Appl. 42 (2017) 775–787.
[21] S.W. Hsiao, M.H. Yang, A methodology for predicting the color trend to get a three-colored combination, Color Res. Appl. 42 (2017) 102–114.
[22] H.-C. Tsai, Chou, J.-R, Automatic design support and image evaluation of two-coloured products using colour association and colour harmony scales and genetic algorithm, Comput. Aided Des. 39 (2007) 818–828.
[23] S. Takamoto, T. Yamasaki, J. Nara, T. Ohno, C. Kaneta, A. Hatano, S. Izumi, Atomistic mechanism of graphene growth on a SiC substrate: Large-scale molecular dynamics simulations based on a new charge-transfer bond-order type potential, Phys. Rev. B 97 (2018).
[24] S.W. Hsiao, M.F. Wang, D.J. Lee, C.W. Chen, A study on the application of an artificial neural algorithm in the color matching of taiwanese cultural and creative commodities, Color Res. Appl. 40 (2015) 341–351.
[25] S.W. Hsiao, H.C. Tsai, Use of gray system theory in product-color planning, Color Res. Appl. 29 (2004) 222–231.
[26] S.W. Hsiao, M.H. Yang, C.H. Lee, An aesthetic measurement method for matching colours in product design, Color Res. Appl. 42 (2017) 664–683.
[27] P. Choi, S. Orsborn, P. Boatwright, Bayesian analysis of color preferences: An application for product and product line design, Color Res. Appl. 41 (2016) 445–456.
[28] C.Y. Lee, J.J. Leou, H.H. Hsiao, Saliency-directed color image segmentation using modified particle swarm optimization, Signal Process. 92 (2012) 1–18.
[29] I.H. Hsiao, Y.L. Lin, Cyber Java Monopoly: Game-Based Approach of Collaborative Programming Language Learning, Iconference, 2011.
[30] C.-f. Shiu, The Application of Neural Network on Color and Image Predicting Model for Children Product, National Cheng Kung University, Taiwan, 2007.
[31] H.-Y. Chen, Chang, Y.-M, Extraction of product form features critical to determining consumers' perceptions of product image using a numerical definition-based systematic approach, Int. J. Ind. Ergon. 39 (2009) 133–145.
[32] M.S. Li, S.Y. Lian, F. Wang, Y.Y. Zhou, B.S. Chen, L.X. Guan, Y. Wu, Prediction model of organic molecular absorption energies based on deep learning trained by chaos-enhanced accelerated evolutionary algorithm, Sci. Rep. 9 (2019) 17261.
[33] K. Sayevand, H. Arab, A fresh view on particle swarm optimization to develop a precise model for predicting rock fragmentation, Eng. Comput. 36 (2019) 533–550.
[34] S.W. Du, Y. Li, A novel deformation forecasting method utilizing comprehensive observation data, Adv. Mech. Eng. 10 (2018).

Mengshan Li

Suyun Lian

Fan Wang

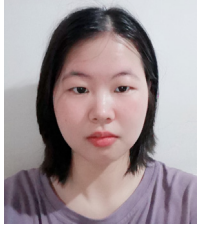

Yanying Zhou

Bingsheng Chen

Lixin Guan

Yan Wu